Link between the Superconducting Dome and Spin-Orbit Interaction in the (111) $LaAlO_3/SrTiO_3$ Interface

P. K. Rout, E. Maniv, and Y. Dagan*

Raymond and Beverly Sackler School of Physics and Astronomy, Tel-Aviv University, Tel Aviv 69978, Israel

(Received 6 June 2017; published 4 December 2017)

We measure the gate voltage (V_g) dependence of the superconducting properties and the spin-orbit interaction in the (111)-oriented $LaAlO_3/SrTiO_3$ interface. Superconductivity is observed in a dome-shaped region in the carrier density-temperature phase diagram with the maxima of superconducting transition temperature T_c and the upper critical fields lying at the same V_g. The spin-orbit interaction determined from the superconducting parameters and confirmed by weak-antilocalization measurements follows the same gate voltage dependence as T_c. The correlation between the superconductivity and spin-orbit interaction as well as the enhancement of the parallel upper critical field, well beyond the Chandrasekhar-Clogston limit, suggest that superconductivity and the spin-orbit interaction are linked in a nontrivial fashion. We propose possible scenarios to explain this unconventional behavior.

DOI: 10.1103/PhysRevLett.119.237002

Oxide heterostructures provide unique platform where various degrees of freedom from the constituent materials can combine such that new collective phenomena emerge at the interfaces [1]. An interesting example is a two-dimensional (2D) electron liquid at the interface between (100)-oriented $SrTiO_3$ and $LaAlO_3$ that exhibits gate tunable superconductivity [2–4] and spin-orbit interaction [4–6]. Recent experiments on (111) $LaAlO_3/SrTiO_3$ have shown 2D conduction [7–9] and superconductivity with a transition temperature (T_c) of about 100 mK [10,11]. In a (111)-oriented $LaAlO_3/SrTiO_3$ interface, the cubic lattice is projected onto the (111) plane of the interface, resulting in a 2D sixfold crystalline structure. Angle-resolved photoemission studies on the (111) $SrTiO_3$ surface reveal a sixfold symmetric electronic structure [12,13]. This 2D crystalline symmetry is also reflected in the magnetotransport properties [9] and has been predicted to host exotic electronic orders [14–17]. At low temperatures, this symmetry is lowered, since bulk $SrTiO_3$ undergoes multiple structural transitions. Below 105 K, a transition from a cubic to a tetragonal phase occurs [18]. The symmetry is further reduced to triclinic below ~70 K, and polar domain walls where inversion symmetry is broken are created [19]. Such a domain wall can be pinned to the interface, resulting in unconventional superconductivity, which is linked to spin-orbit coupling.

In a 2D superconductor, for a magnetic field applied perpendicular to the superconducting plane, superconductivity is broken when vortices become closely packed. By contrast, the parallel upper critical field ($H_{c\parallel}$) is determined by the Chandrasekhar-Clogston limit [20,21], which is set by comparing the Zeeman energy to the superconducting gap. In the presence of a spin-orbit interaction, this upper bound is relaxed [22,23].

In this Letter, we report a nonmonotonic (dome-shaped) dependence of T_c with a gate voltage in the (111) $SrTiO_3/LaAlO_3$ interfaces. From the gate dependence of T_c and $H_{c\parallel}$, we estimate the spin-orbit energy (ε_{SO}), which follows the nonmonotonic behavior of T_c. Remarkably, we found similar behavior for the spin-orbit field H_{SO} extracted from weak antilocalization measurements.

Epitaxial films of $LaAlO_3$ were deposited on an atomically flat $SrTiO_3$ (111) substrate using pulsed laser deposition. The details of the deposition procedure and substrate treatment are described in Ref. [9]. We control the layer-by-layer growth of 14 monolayers (LaO_3/Al layers) by reflection high-energy electron diffraction oscillations. The atomic force microscope images show the step and terrace morphology of the film with step heights of 0.22 nm. The electrical measurements with the current along the $[11\bar{2}]$ direction were carried out in a Leiden Cryogenics custom-made dilution refrigerator.

Figure 1(a) presents the temperature-dependent sheet resistance R_S (T) at various gate voltages V_g. A clear gate-dependent superconducting transition is observed. We define the critical temperature T_c as the temperature at which R_S reaches half of its value at 350 mK. The normal state resistance R_S (350 mK) decreases monotonically with increasing V_g [Fig. 1(b)], which is consistent with previous reports [8,9]. The monotonic increase of R_S is contrasted with the nonmonotonic dependence of T_c on V_g. A similar dome-shaped region in the carrier density-temperature phase diagram is seen in many unconventional superconductors and in the (100) $LaAlO_3/SrTiO_3$ interface.

In the (100) $LaAlO_3/SrTiO_3$ interface, the Hall coefficient depends nonmonotonically on the gate voltage. Surprisingly, this nonmonotonic behavior is also seen in the gate dependence of the Shubnikov–de Haas oscillation (SdH) frequency. Both the SdH frequency and low field inverse Hall coefficient follow the gate dependence of T_c for the (100) interface [3,24], or the superconductivity starts

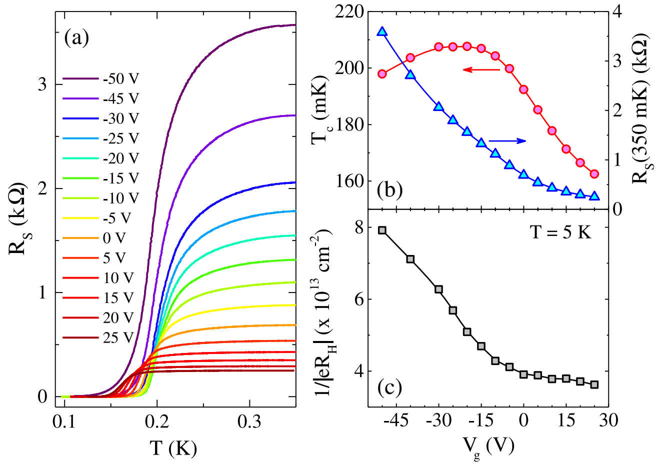

FIG. 1. (a) Temperature dependence of sheet resistance R_S (T) for various gate voltages. (b) T_c and R_S (350 mK) as a function of V_g. (c) Gate dependence of the inverse Hall coefficient $1/|eR_H|$ at $T = 5$ K.

appearing when the low field inverse Hall coefficient decreases from its maximum value [25]. By contrast, for the (111) interface the inverse Hall coefficient monotonically decreases with V_g [Fig. 1(c)] consistent with previous observations [8,9]. In the case of the (111) $LaAlO_3/SrTiO_3$ interface, the titanium t_{2g} bands are split into low and high spin states due to the atomic spin-orbit interaction [14,15]. We have shown that the lower spin state is first populated when accumulating electrons with increasing V_g [9]. This two-band scenario complicates the interpretation of the Hall data. We have estimated the amount of carrier density modulation due to the electric field effect similar to Refs. [2,26]. Since the V_g range used is relatively small, the nonlinearities in the dielectric constant (ϵ) can be neglected, and thus the corresponding modulation of electron density is $\simeq 1.3 \times 10^{13}$ cm^{-2} with $\epsilon \simeq 15000$. This value is much smaller than the net change in $1/|eR_H|$ of $\simeq 4.3 \times 10^{13}$ cm^{-2}. Moreover, the electron density due to the field effect increases with V_g in contrast to the observed behavior in Fig. 1(c). All these observations indicate the presence of a hole band in addition to electron band(s) in the (111) interface. We have confirmed this scenario by analyzing the normal state transport data via a simplistic noninteracting two-band model with one hole and one electron band (see Ref. [27] for more details). Therefore, it is possible that the hole contribution to the electronic transport (and perhaps to superconductivity) becomes important in this V_g range [8]. This is also consistent with the polar structure of the (111) interface [7].

The sheet resistance versus magnetic field at 90 mK for various gate voltages is plotted in Figs. 2(a) and 2(b) for perpendicular and parallel field configurations, where the sample is properly aligned with the field within an accuracy of 2°. We define the critical field ($H_{c\perp}$) for the perpendicular magnetic field configuration such that $R_S(H_{c\perp}) = R_S(350\text{ mK})/2$, and a similar criterion is followed for $H_{c\parallel}$ [28]. In Fig. 2(c), we plot $H_{c\parallel}$ and $H_{c\perp}$ as a function of V_g, both exhibiting nonmonotonic

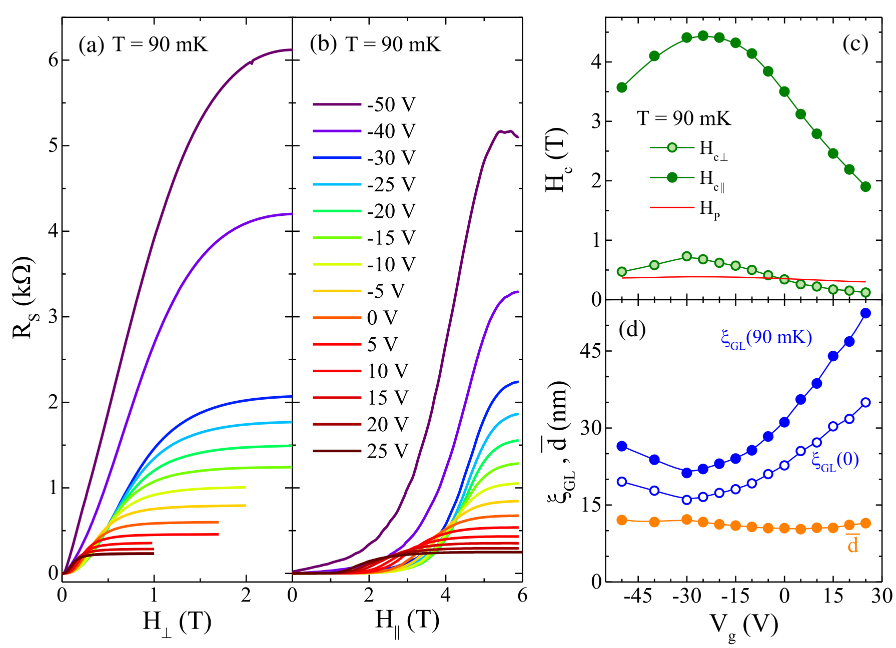

FIG. 2. Magnetoresistance R_S (H) at $T = 90$ mK in (a) perpendicular ($\vec{H}$ perpendicular to the current and interface) and (b) longitudinal ($\vec{H}$ parallel to the current and interface) configurations for various V_g. (c) $H_{c\perp}$ and $H_{c\parallel}$ at 90 mK as a function of V_g along with the Chandrasekhar-Clogston limit H_P. (d) Gate dependence of ξ_{GL} (90 mK), $\xi_{\mathrm{GL}}(0)$, and $\bar{d}$.

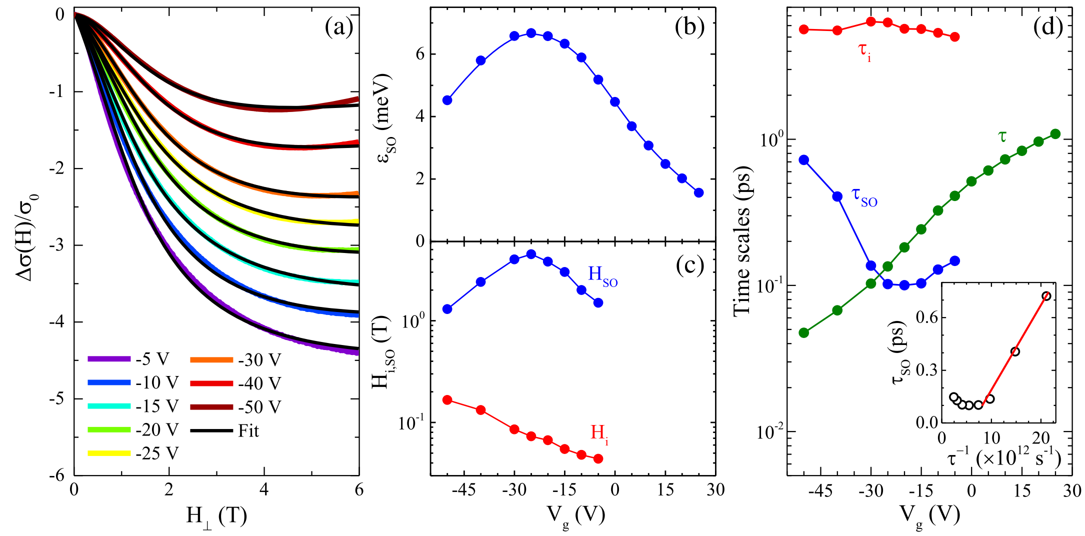

FIG. 3. (a) The normalized perpendicular magnetoconductance $\Delta\sigma(H)/\sigma_0$ for different V_g at $T = 1.3$ K. The black solid lines are the fits according to Eq. (1). (b) ε_{SO} as a function of V_g determined from $H_{c\parallel}$ (see the text for more details). (c) Gate dependence of H_i and H_{SO} extracted from the fitting of weak antilocalization. (d) Gate dependence of τ_i, τ_{SO}, and τ. The inset shows τ_{SO} as a function of τ^{-1} along with the solid line as a guide to the eye.

behavior with the maximum at the same gate voltage as T_c. $H_{c\parallel} > H_{c\perp}$ for all gate voltages reaching a maximal ratio of $\sim$16. Such strong anisotropy between two field orientations is evidence for 2D superconductivity in the (111) interface. Thus, it is expected that the superconducting layer thickness (d) should be smaller than the Ginzburg-Landau coherence length (ξ_{GL}). To check this, we extract ξ_{GL} from $H_{c\perp}$ using the relation $\xi_{GL} = \sqrt{\Phi_0/2\pi H_{c\perp}}$. It is presented in Fig. 2(d) together with its extrapolation to zero temperature using $H_{c\perp}(T) = H_{c\perp}(0)(1 - T/T_c)$ valid for a 2D superconductor. Since the parallel magnetic field fully penetrates a 2D ($d \ll \xi$) superconductor, we can only estimate the upper limit for d denoted as $\bar{d}$, which can be found from $\bar{d} = \sqrt{3}\Phi_0/\pi\xi_{GL}H_{c\parallel}$ [see Fig. 2(d)]. We note that, for all V_g, $\bar{d} < \xi_{GL}(0)$, rendering superconductivity in the (111) $SrTiO_3/LaAlO_3$ two dimensional.

For a parallel field configuration in a 2D superconductor, the orbital motion and vortices can be neglected, making the Zeeman energy the dominant pair-breaking effect. This leads to an upper (Chandrasekhar-Clogston) limit of $H_{c\parallel}$ given by $H_P = 3.5k_BT_c/\sqrt{2}g\mu_B$ (μ_B is the Bohr magneton) in the BCS weak coupling limit [20,21]. Assuming a gyromagnetic ratio of $g \simeq 2$, we observe $H_{c\parallel} > H_P$ for all gate voltages reaching a maximal ratio of $\sim$11 [Fig. 2(c)]. In the presence of strong spin-orbit coupling, the Chandrasekhar-Clogston limit can be relaxed. Other reasons for breaking this limit could be strong coupling superconductivity, many-body effects, and an anisotropic pairing mechanism.

To determine the spin-orbit interaction from $H_{c\parallel}$, we use a somewhat oversimplified picture of spin-orbit scattering that suppresses spin orientation by the Zeeman field [22]. For a strong spin-orbit interaction, $H_{c\parallel}$ can be expressed in terms of the spin-orbit energy (ε_{SO}) as $H_{c\parallel} = 0.602\sqrt{\varepsilon_{SO}/k_BT_c}H_P$ with $\varepsilon_{SO} = \hbar/\tau_{SO}$, and τ_{SO} is the spin-orbit scattering time. Remarkably, this analysis reveals a nonmonotonic dependence of ε_{SO} on V_g as shown in Fig. 3(b). This is the main finding of our Letter. For (110) $LaAlO_3/SrTiO_3$, gate-independent spin-orbit coupling has been observed [29], perhaps because of the nonpolar structure of this interface. The findings on the (110) interface are contrasted with our results of a strong and gate-tunable spin-orbit interaction for the (111) interface that follows the behavior of the superconducting dome. A weaker correlation between spin-orbit coupling and T_c in the (100) interface can be deduced by combining Refs. [4–6], where $H_{c\parallel}$ is smaller.

To further confirm the presence of a spin-orbit interaction, we studied the perpendicular magnetoresistance well above T_c at 1.3 K [Fig. 3(a)]. For a 2D diffusive metallic system placed in a perpendicular magnetic field (H), the field-dependent quantum correction to conductivity $\Delta\sigma(H)$ normalized by quantum conductance ($\sigma_0 = 2e^2/h$) can be expressed as [5,30]

$$\begin{aligned}\frac{\Delta\sigma(H)}{\sigma_0} = {}& \Psi\left(\frac{H}{H_i + H_{SO}}\right) \\ &+ \frac{1}{2\sqrt{1-\gamma^2}}\Psi\left(\frac{H}{H_i + H_{SO}(1+\sqrt{1-\gamma^2})}\right) \\ &- \frac{1}{2\sqrt{1-\gamma^2}}\Psi\left(\frac{H}{H_i + H_{SO}(1-\sqrt{1-\gamma^2})}\right) \\ &- \frac{AH^2}{1+CH^2}, \qquad (1)\end{aligned}$$

where $\Psi(x) = \ln(x) + \psi[\frac{1}{2} + (1/x)]$ [$\psi(x)$ is the digamma function] and $\gamma = g\mu_B H/4eDH_{SO}$ (D is the diffusion coefficient). H_i and H_{SO} are the inelastic and spin-orbit fields, respectively. The classical orbital magnetoresistance contributes a Kohler term to Eq. (1) with the parameters A and C. Figure 3(c) shows H_i and H_{SO} for different V_g (see Supplemental Material for the gate dependence of g, A, and C [27]). Clearly, $H_{SO} > H_i$ for all V_g, suggesting that we are in the weak antilocalization regime [see Fig. 3(a)]. H_{SO} from weak antilocalization [Fig. 3(c)] shows nonmonotonic behavior similar to ε_{SO} inferred from superconductivity [Fig. 3(b)], and, furthermore, they have a maximum value at the same gate voltage as T_c.

In general, the $LaAlO_3/SrTiO_3$ interface has a complicated band structure involving multiple contributions from the titanium d bands [31,32]. Therefore, the extracted parameters from weak antilocalization do not correspond to an individual band; instead, an averaged value over all the bands should be considered [33]. We have extracted various averaged time scales, i.e., τ_{SO}, τ_i (inelastic time), and τ (elastic scattering time) [Fig. 3(d)]. The $\tau_{SO(i)}$ are related to $H_{SO(i)}$ determined from weak antilocalization as $H_{SO(i)} = \hbar/4eD\tau_{SO(i)}$. The effective diffusion coefficient (D) and τ are calculated using a naïve Drude model for a 2D electron gas (see Ref. [27]). Using this analysis, we find that τ_{SO} depends linearly on τ^{-1} for $V_g < -25$ V [see the inset in Fig. 3(d)], while for $V_g > -25$ V both τ_{SO} and τ increase with V_g [Fig. 3(d)].

The low V_g regime ($V_g < -25$ V) is governed by a D'yakonov-Perel'-type spin-orbit relaxation mechanism for which $\tau_{SO} \propto \tau^{-1}$. In this scenario, the electron precesses around the spin-orbit field, which is changing due to momentum scattering at a typical time τ [34]. The high V_g regime, on the other hand, is characterized by $\tau_{SO} \propto \tau$, suggesting that the electron spin is coupled to the crystal momentum. Interestingly, these two regimes separated by the point where $\tau_{SO} \simeq \tau$ and the maximum of T_c (and $H_{c\parallel}$) dome lies close to this V_g. All these observations suggest the mixing of multiple bands in the presence of a strong spin-orbit interaction for higher V_g. This scenario concurs with our recent report of crystalline sixfold anisotropic magnetoresistance in the (111) interfaces [9], where the sixfold term appears as a result of another band with higher spin state J getting populated with increasing V_g. It is therefore possible that the crystalline spin-orbit interaction becomes important close to this avoided band crossing region due to the orbital mixing [23,35]. This interaction becomes smaller as V_g is further increased away from the band crossing regime, resulting in a dome in the spin-orbit energy versus V_g. Such a multiband effect can also lead to dome-shaped superconductivity with maximum T_c lying at this regime [as observed in Fig. 1(b)] similar to the case for the (100) interface [3]. A more exotic mechanism of superconductivity in the $LaAlO_3/SrTiO_3$ interface involves the formation of a Fulde-Ferrell-Larkin-Ovchinikov (FFLO) state due to large spin-orbit coupling [36]. This can somewhat explain the nonmonotonic gate dependence of $H_{c\parallel}$ and T_c with the maxima lying at $\tau_{SO} = \tau$. However, the $H_{c\parallel}$ for a quasi-2D superconductor in a FFLO state is estimated to be at most 2.5 times the Chandrasekhar-Clogston limit [37], which is much lower than the observed values [see Fig. 2(c)]. Therefore, a full theoretical understanding of the phenomenological link observed here between the superconducting dome and the spin-orbit energy is yet to be developed.

Salje *et al.* have found that for $SrTiO_3$ below ~70 K the tetragonal symmetry is lowered and the Sr atoms are displaced along the [111] direction, leading to the breaking of local inversion symmetry [19]. It is therefore possible that a (111) $SrTiO_3$-based polar interface has such broken inversion symmetry in addition to conventional inversion symmetry breaking observed at polar oxide interfaces, which can result in an unconventional superconductivity. It has been recently suggested that dichalcogenide monolayers with hexagonal structure can be a realization of exotic Ising superconductivity where the spins are locked in an out-of-plane configuration due to the breaking of centrosymmetry [38–40]. We also note that the possibility for a nodeless time-reversal-symmetry-breaking superconducting order parameter has been proposed for (111) $SrTiO_3$-based interfaces from symmetry considerations [16].

In summary, the superconducting transition temperature T_c of the (111) $LaAlO_3/SrTiO_3$ interface has a nonmonotonic dependence on the gate voltage. Maximum T_c is found at the same gate voltage where maximal values of spin-orbit field H_{SO} and spin-orbit energy ε_{SO} are observed. H_{SO} is extracted from weak antilocalization, while ε_{SO} is estimated from the superconducting properties. The $H_{c\parallel}$ exceeds the Chandrasekhar-Clogston limit by more than an order of magnitude due to a strong spin-orbit interaction. We suggest that the crystalline spin-orbit interaction becomes important close to an avoided band crossing region. In this regime, orbital mixing can lead to enhanced spin-orbit interaction and superconductivity, which become weaker as V_g is tuned away from this avoided band crossing regime. This results in a dome in the spin-orbit energy (and T_c) versus V_g. However, a deeper insight to the link between spin-orbit interaction and the superconducting dome requires a further development of theoretical models for this unique hexagonal oxide interface.

We are indebted to Moshe Goldstein and Alexander Palevski for useful discussions. This work has been supported by the Israel Science Foundation under Grant No. 382/17, the Israel Ministry of Science technology and space under Contract No. 3-11875, and the Bi-national science foundation under Grant No. 2014047.

P. K. R. and E. M. contributed equally to this work.

*yodagan@post.tau.ac.il

[1] H. Y. Hwang, Y. Iwasa, M. Kawasaki, B. Keimer, N. Nagaosa, and Y. Tokura, Nat. Mater. **11**, 103 (2012).
[2] A. Caviglia, S. Gariglio, N. Reyren, D. Jaccard, T. Schneider, M. Gabay, S. Thiel, G. Hammerl, J. Mannhart, and J.-M. Triscone, Nature (London) **456**, 624 (2008).
[3] E. Maniv, M. B. Shalom, A. Ron, M. Mograbi, A. Palevski, M. Goldstein, and Y. Dagan, Nat. Commun. **6**, 8239 (2015).
[4] M. Ben Shalom, M. Sachs, D. Rakhmilevitch, A. Palevski, and Y. Dagan, Phys. Rev. Lett. **104**, 126802 (2010).
[5] A. D. Caviglia, M. Gabay, S. Gariglio, N. Reyren, C. Cancellieri, and J.-M. Triscone, Phys. Rev. Lett. **104**, 126803 (2010).
[6] H. Liang, L. Cheng, L. Wei, Z. Luo, G. Yu, C. Zeng, and Z. Zhang, Phys. Rev. B **92**, 075309 (2015).
[7] G. Herranz, F. Sánchez, N. Dix, M. Scigaj, and J. Fontcuberta, Sci. Rep. **2**, 758 (2012).
[8] S. Davis, V. Chandrasekhar, Z. Huang, K. Han, Ariando, and T. Venkatesan, Phys. Rev. B **95**, 035127 (2017).
[9] P. K. Rout, I. Agireen, E. Maniv, M. Goldstein, and Y. Dagan, Phys. Rev. B **95**, 241107 (2017).
[10] A. M. R. V. L. Monteiro, D. J. Groenendijk, I. Groen, J. de Bruijckere, R. Gaudenzi, H. van der Zant, and A. Caviglia, Phys. Rev. B **96**, 020504 (2017).
[11] S. Davis, Z. Huang, K. Han, Ariando, T. Venkatesan, and V. Chandrasekhar, arXiv:1704.01203.
[12] S. McKeown Walker, A. de la Torre, F. Y. Bruno, A. Tamai, T. K. Kim, M. Hoesch, M. Shi, M. S. Bahramy, P. D. C. King, and F. Baumberger, Phys. Rev. Lett. **113**, 177601 (2014).
[13] T. C. Rödel *et al.*, Phys. Rev. Applied **1**, 051002 (2014).
[14] D. Xiao, W. Zhu, Y. Ran, N. Nagaosa, and S. Okamoto, Nat. Commun. **2**, 596 (2011).
[15] D. Doennig, W. E. Pickett, and R. Pentcheva, Phys. Rev. Lett. **111**, 126804 (2013).
[16] M. S. Scheurer, D. F. Agterberg, and J. Schmalian, npj Quantum Mater. **2**, 9 (2017).
[17] S. Okamoto and D. Xiao, arXiv:1705.05683.
[18] K. A. Müller and H. Burkard, Phys. Rev. B **19**, 3593 (1979).
[19] E. K. H. Salje, O. Aktas, M. A. Carpenter, V. V. Laguta, and J. F. Scott, Phys. Rev. Lett. **111**, 247603 (2013).
[20] B. Chandrasekhar, Appl. Phys. Lett. **1**, 7 (1962).
[21] A. M. Clogston, Phys. Rev. Lett. **9**, 266 (1962).
[22] R. A. Klemm, A. Luther, and M. Beasley, Phys. Rev. B **12**, 877 (1975).
[23] Y. Nakamura and Y. Yanase, J. Phys. Soc. Jpn. **82**, 083705 (2013).
[24] A. E. M. Smink, J. C. de Boer, M. P. Stehno, A. Brinkman, W. G. van der Wiel, and H. Hilgenkamp, Phys. Rev. Lett. **118**, 106401 (2017).
[25] G. Singh *et al.*, arXiv:1704.03365.
[26] J. Biscaras, N. Bergeal, S. Hurand, C. Grossetête, A. Rastogi, R. C. Budhani, D. LeBoeuf, C. Proust, and J. Lesueur, Phys. Rev. Lett. **108**, 247004 (2012).
[27] See Supplemental Material at http://link.aps.org/supplemental/10.1103/PhysRevLett.119.237002 for more details about the two-band model for Hall data and the analysis of weak antilocalization.
[28] For $V_g \leq -40$ V, the saturation resistance at a high field is significantly larger than the resistance at 350 mK (above T_c). But these two quantities coincide for other gate voltages. This may be related to the proximity to a superconductor-to-insulator transition for lower V_g and will be discussed elsewhere.
[29] G. Herranz *et al.*, Nat. Commun. **6**, 6028 (2015).
[30] S. Maekawa and H. Fukuyama, J. Phys. Soc. Jpn. **50**, 2516 (1981).
[31] M. Ben Shalom, A. Ron, A. Palevski, and Y. Dagan, Phys. Rev. Lett. **105**, 206401 (2010).
[32] S. Lerer, M. Ben Shalom, G. Deutscher, and Y. Dagan, Phys. Rev. B **84**, 075423 (2011).
[33] D. Rainer and G. Bergmann, Phys. Rev. B **32**, 3522 (1985).
[34] I. Žutić, J. Fabian, and S. Das Sarma, Rev. Mod. Phys. **76**, 323 (2004).
[35] Z. Zhong, A. Tóth, and K. Held, Phys. Rev. B **87**, 161102 (2013).
[36] K. Michaeli, A. C. Potter, and P. A. Lee, Phys. Rev. Lett. **108**, 117003 (2012).
[37] H. Shimahara, J. Phys. Soc. Jpn. **66**, 541 (1997).
[38] J. Lu, O. Zheliuk, I. Leermakers, N. F. Yuan, U. Zeitler, K. T. Law, and J. Ye, Science **350**, 1353 (2015).
[39] X. Xi, Z. Wang, W. Zhao, J.-H. Park, K. T. Law, H. Berger, L. Forró, J. Shan, and K. F. Mak, Nat. Phys. **12**, 139 (2016).
[40] Y. Saito *et al.*, Nat. Phys. **12**, 144 (2016).